Free Radical Research, July 2011; 45(7): 848–857

informa
healthcare

Aldo-keto reductase 1C15 as a quinone reductase in rat endothelial cell: Its involvement in redox cycling of 9,10-phenanthrenequinone

TOSHIYUKI MATSUNAGA[1], YUHKI SHINODA[1], YUKARI INOUE[1], YUKI SHIMIZU[1], MARIKO HAGA[1], SATOSHI ENDO[1], OSSAMA EL-KABBANI[2] & AKIRA HARA[1]

[1]*Laboratory of Biochemistry, Gifu Pharmaceutical University, Gifu 501-1196, Japan, and* [2]*Medicinal Chemistry and Drug Action, Monash Institute of Pharmaceutical Sciences, Monash University, Parkville, Victoria 3052, Australia*

(Received date: 24 March 2011; Accepted date: 22 April 2011)

Abstract

9,10-Phenanthrenequinone (9,10-PQ), a redox-active quinone in diesel exhausts, triggers cellular apoptosis via reactive oxygen species (ROS) generation in its redox cycling. This study found that induction of CCAAT/enhancer-binding protein-homologous protein (CHOP), a pro-apoptotic factor derived from endoplasmic reticulum stress, participates in the mechanism of rat endothelial cell damage. The 9,10-PQ-mediated CHOP induction was strengthened by a proteasome inhibitor (MG132) and the MG132-induced cell sensitization to the 9,10-PQ toxicity was abolished by a ROS inhibitor, suggesting that ROS generation and consequent proteasomal dysfunction are responsible for the CHOP up-regulation caused by 9,10-PQ. Aldo-keto reductase (AKR) 1C15 expressed in rat endothelial cells reduced 9,10-PQ into 9,10-dihydroxyphenanthrene concomitantly with superoxide anion formation, implying its participation in evoking the 9,10-PQ-redox cycling. The 9,10-PQ-induced damage was augmented by AKR1C15 over-expression. 9,10-PQ also provoked the AKR1C15 up-regulation, which sensitized against the quinone toxicity. These results suggest the presence of a negative feedback loop exacerbating the quinone toxicity in rat endothelial cells.

Keywords: *9,10-Phenanthrenequinone, aldo-keto reductase 1C15, redox cycling, oxidative stress, endoplasmic reticulum stress*

Abbreviations: *AKR, aldo-keto reductase; BAE, bovine aortic endothelial; CHOP, CCAAT/enhancer-binding protein-homologous protein; CuZnSOD, copper, zinc-superoxide dismutase; 9,10-DAP, 9,10-diacetoxyphenanthrene; DEP, diesel exhaust particles; DMEM, Dulbecco's modified Eagle medium; DMSO, dimethylsulphoxide; DPBS, Dulbecco's phosphate-buffered saline; ER, endoplasmic reticulum; FBS, foetal bovine serum, 4HNE, 4-hydroxy-2-nonenal; Keap1, Kelch-like ECH-associated protein 1; Nrf2, nuclear factor erythroid 2-related factor 2; 8-OHdG, 8-hydroxydeoxyguanosine; PARP, poly(ADP-ribose) polymerase; 9,10-PQ, 9,10-phenanthrenequinone; 9,10-PQH$_2$, 9,10-dihydroxyphenanthrene; PEG-cat, polyethylene glycol-conjugated catalase; PERK, double stranded RNA-activated protein kinase-like endoplasmic reticulum kinase; ROS, reactive oxygen species.*

Introduction

Chronic inhalation of urban air pollutants is thought to be a major risk factor for respiratory diseases, including asthma, bronchitis and carcinoma [1–4]. Among the pollutants, particle matters under 2.5 μm such as diesel exhaust particles (DEP) not only easily reach pulmonary alveoli but also accumulate throughout the lungs, thereby leading to severe inflammatory disorders [5,6]. In addition, the particles seem to enter the systemic circulation and to cause vascular cell injury [7–9]. DEP consist of a carbon core and the surrounding organic components, such as polycyclic aromatic hydrocarbons, nitroaromatic hydrocarbons, heterocyclics, aldehydes and quinones [10]. One of the most toxic compounds found in DEP is 9,10-phenanthrenequinone (9,10-PQ), which is considered to induce apoptotic cell death [11] mainly due to excessive generation of reactive oxygen species

Correspondence: Toshiyuki Matsunaga, Laboratory of Biochemistry, Gifu Pharmaceutical University, 1-25-4 Daigaku-nishi, Gifu, 501-1196, Japan. Tel: +81-58-230-8100. Fax: +81-58-230-8105. Email: matsunagat@gifu-pu.ac.jp

ISSN 1071-5762 print/ISSN 1029-2470 online
DOI: 10.3109/10715762.2011.585648

(ROS) in its redox cycling [12–14]. The 9,10-PQ redox cycling is initiated by reduction of the *o*-quinone by NADPH-dependent reductases, in which the resulting 9,10-dihydroxyphenanthrene (9,10-PQH_2) is rapidly converted into 9,10-PQ through its semiquinone radical in the presence of molecular oxygen, concomitantly with generation of ROS such as superoxide anion and hydrogen peroxide. Previous studies proposed NADPH-cytochrome P450 reductase [15,16] and carbonyl reductase [12,13] as potential reductases involved in the redox cycling. In addition, we recently found that L-xylulose reductase and aldo-keto reductase (AKR) 1C3 function as the predominant 9,10-PQ reductases in human T-lymphoma [17] and endothelial cells [18], respectively.

The AKR superfamily is comprised of more than 140 members that are in general cytosolic NAD(P)(H)-dependent oxidoreductases for a variety of carbonyl compounds including endogenous carbohydrates, steroids and prostaglandins [19]. The oxidoreductases of steroids and prostaglandins belong to the AKR1C subfamily of this superfamily. While the human members of this subfamily are four AKRs (1C1, 1C2, 1C3 and 1C4), seven members are present in rat tissues and named AKR1C8, AKR1C9, AKR1C15, AKR1C16, AKR1C17, AKR1C24 and RAKh (17β-hydroxysteroid dehydrogenase). Among the rat AKR1C subfamily members, AKR1C15 is unique in its high expression in the vascular endothelial cells and epithelial cells of respiratory and digestive organs [20]. The enzyme is a monomeric NADPH-dependent reductase with a molecular weight of 36-kDa and its outstanding feature is the broad substrate specificity for aromatic, alicyclic and aliphatic carbonyl compounds, including 17-ketosteroids, monosaccharides and lipid-derived aldehydes. We recently found that AKR1C15 is capable of lessening cytotoxicity of 4-hydroxy-2-nonenal (4HNE), a reactive lipid metabolite formed in oxidative stress, by reducing into less toxic 1,4-dihydroxy-2-nonene [21]. On the other hand, AKR1C15 efficiently reduces 9,10-PQ, showing *K*m and *k*cat/*K*m (catalytic efficiency) of 0.6 μM and 43 $min^{-1}\mu M^{-1}$, respectively [20]. Since the kinetic constants for 9,10-PQ are comparable to those of human L-xylulose reductase and AKR1C3 [17,18], it is expected that AKR1C15 acts as a key enzyme undergoing the redox cycling of 9,10-PQ that consequently induces the toxic effect of the quinone on rat endothelial cells.

In this study, we have inquired into the possible mechanism(s) underlying the 9,10-PQ-induced damage of rat endothelial YPEN1 cells and found that its treatment provokes the apoptosis through the enhanced ROS production and subsequent endoplasmic reticulum (ER) stress induction. In addition, our analyses of the enzymology and molecular biology of endothelial cell damage caused by 9,10-PQ show that AKR1C15 plays a major role in the ROS production through the redox cycling of the quinone. Furthermore, we show for the first time the induction of AKR1C15 by oxidative stress evoked by 9,10-PQ.

Methods

Chemicals and enzymes

9,10-PQ and a protein transfection reagent, Profect P-2, were purchased from Nacalai Tesque (Kyoto, Japan). TRIzol reagent and Lipofectamine 2000 transfection reagent were obtained from Invitrogen (Carlsbad, CA); acetyl Asp-Glu-Val-Asp *p*-nitroanilide and acetyl Leu-Glu-His-Asp *p*-nitroanilide were from Sigma-Aldrich (St. Louis, MO); 8-hydroxydeoxyguanosine (8-OHdG) enzyme-linked immunosorbent assay kit was from Japan Institute for the Control and Aging (Shizuoka, Japan); bicinchoninic acid protein assay system was from Pierce (Rockford, IL); and enhanced chemiluminescence substrate system was from Amersham Biosciences (Piscataway, NJ). *Taq* DNA polymerase and copper, zinc-superoxide dismutase (CuZnSOD) were obtained from Takara (Kusatsu, Japan) and UBE industrials (Tokyo, Japan), respectively. Polyethylene glycol-conjugated catalase (PEG-cat) and 9,10-diacetoxyphenanthrene (9,10-DAP) were generously gifted from Dr Yoshito Kumagai (University of Tsukuba, Japan). The recombinant AKR1C15 was expressed from an expression plasmid harbouring its cDNA and purified to homogeneity as described previously [20]. All other chemicals were of the highest grade that could be obtained commercially.

Culture of cells and tissues

Rat prostate endothelial YPEN1 cells were obtained from American Type Culture Collection (Manassas, VA). Bovine aortic endothelial (BAE) cells were generously gifted from Dr Junichi Nakagawa (Tokyo University of Agriculture, Abashiri, Japan). The cells were cultured in Dulbecco's modified Eagle medium (DMEM) supplemented with 10% foetal bovine serum (FBS), penicillin (100 U/ml) and streptomycin (100 μg/ml) at 37°C in a humidified incubator containing 5% CO_2, except that 1 mM sodium pyruvate, 0.1 mM non-essential amino acids and 0.03 mg/ml heparin were additionally supplemented in the culture medium of YPEN1 cells. In the majority of experiments using the endothelial cells, the cells were used at passage 4–8 and the endothelial cobblestone morphology was confirmed microscopically before use.

Tissues of rat aortic rings and heart were cultured according to the method of Domenighetti et al. [22] with a minor modification. Briefly, masses of the abdominal aortic rings and myocardium were excised in a sterile manner from 16-week-old Wistar male rats. After gently removing adventitia, the tissues were washed sufficiently with medium 199 containing 20% FBS and 50 μg/ml gentamycin to remove blood cells

and cultured in the same medium at 37°C in a CO_2 incubator, except that myocardial tissue was carefully trimmed with fine scissors into small pieces (1–2 mm^3) before the culture.

Transfection

The construction of the mammalian pGW1 expression vector harbouring the cDNA for AKR1C15 and its transfection into BAE cells using Lipofectamine 2000 transfection reagent were performed according to the method described previously [21]. The anti-AKR1C15 antibodies [20] were introduced into the cells using Profect P-2 according to the manufacturer's instruction.

Analyses of cell viability, DNA fragmentation and 8-OHdG

Cell viability was evaluated by a tetrazolium dye-based cytotoxicity assay using 2-(4-iodophenyl)-3-(4-nitrophenyl)-5-(2,4-disulfophenyl)-2H-tetrazolium monosodium salt [23]. The DNA fragmentation due to apoptosis was analysed as described previously [24]. In the measurement of 8-OHdG, the cells were washed twice with ice-cold Dulbecco's phosphate-buffered saline (DPBS), resuspended in DPBS containing 0.1% Triton X-100 and homogenized by sonication. The homogenate was centrifuged at 12 000 x g for 15 min and the 8-OHdG concentration in the supernatant was determined using the enzyme-linked immunosorbent assay kit according to the manufacturer's instruction.

Assay of enzyme activity

The activities of caspase-3 and caspase-9 in the cell extracts were measured using acetyl Asp-Glu-Val-Asp *p*-nitroanilide and acetyl Leu-Glu-His-Asp *p*-nitroanilide, respectively, as the substrates [25]. In the preparation of the extract, the cells were washed twice with ice-cold DPBS, suspended in 50 mM HEPES-NaOH, pH 7.4, containing 5 mM 3-[(3-cholamidopropyl) dimethylammonio]-propanesulphonic acid and 5 mM dithiothreitol and homogenized by passing the cell suspension through a 26 gauge needle (20 strokes). The homogenate was centrifuged at 12 000 x *g* for 15 min and the supernatant was subjected to the assay for caspase activities.

The proteolytic (chymotrypsin-like) activity of *26S* proteasome was measured by the method of Thomas et al. [26] with a minor modification. Briefly, the cells were washed twice with buffer I (50 mM Tris-HCl, pH 7.4, supplemented with 2 mM dithiothreitol, 5 mM $MgCl_2$ and 2 mM ATP) and homogenized in buffer I containing 0.25 M sucrose by passing the cell suspension through a 26 gauge needle (20 strokes). The supernatant, obtained by centrifugation (at 12 000 x g for 15 min) of the homogenate, was mixed with the fluorigenic substrate succinyl-Leu-Leu-Val-Tyr-methylcoumarylamide at a final concentration of 50 μM, and incubated at 37°C for 1 h. The amount of the released methylcoumarylamide was measured at excitation and emission wavelengths of 380 and 460 nm, respectively.

Western blot analysis

The cells and tissues were washed with DPBS and homogenized in DPBS containing 0.1% Triton X-100 and 0.3 mM phenylmethanesulphonyl fluoride. The homogenates were centrifuged at 12 000 x *g* for 15 min to remove debris. Nuclear fraction to detect translocation of nuclear factor erythroid 2–related factor 2 (Nrf2) was prepared according to the method reported by Mohan et al. [27]. After their protein concentrations were determined, the extracts (each 40 μg of proteins) were electrophoretically separated on a 7.5% SDS-polyacrylamide gel under reducing conditions and then transferred to a PVDF membrane (Millipore, Bedford, MA) by electroblotting. After blocking with 5% skim milk, the membrane was allowed to react with primary antibodies against poly(ADP-ribose) polymerase (PARP) (Zymed Laboratories, San Francisco, CA), CCAAT/enhancer-binding protein-homologous protein (CHOP) (Santa Cruz Biotechnology, Santa Cruz, CA), Nrf2 (Santa Cruz Biotechnology) and AKR1C15 [20]. The immunoreactive proteins were detected by being reacted with the peroxidase-conjugated secondary antibody, in which the peroxidase activity was visualized by means of the enhanced chemiluminescence substrate system. The densities of the bands were estimated using a GelDoc 2000 and attached program, Quantity One (Bio-Rad, Millan, Italy).

Quantification of 9,10-PQH_2

9,10-PQH_2 was measured by HPLC as its acetyl derivative, 9,10-DAP [14] with a minor modification. The complete reaction mixture consisted of 0.1 M potassium phosphate, pH 7.4, 0.2 mM NADPH, 0.1 mM EDTA, 20 μM 9,10-PQ and the enzyme, in a total volume of 0.5 ml. After incubating at 25°C for 15 min, acetic anhydride (30 μl) was added into the reaction mixture to form 9,10-DAP, followed by heating at 80°C for 5 min. The mixture was deproteinized by adding trichloroacetic acid (2.5%) and centrifugation at 15 000 x g for 15 min. The supernatant (20 μl) was subjected to HPLC analysis using the μBondasphere C_{18} column, which was eluted isocratically with a mobile phase consisting of acetonitrile/1% acetic acid (3:2) at a flow rate of 1 ml/min. The elution of 9,10-PQ and 9,10-DAP was monitored using an ultraviolet detector at 255 nm.

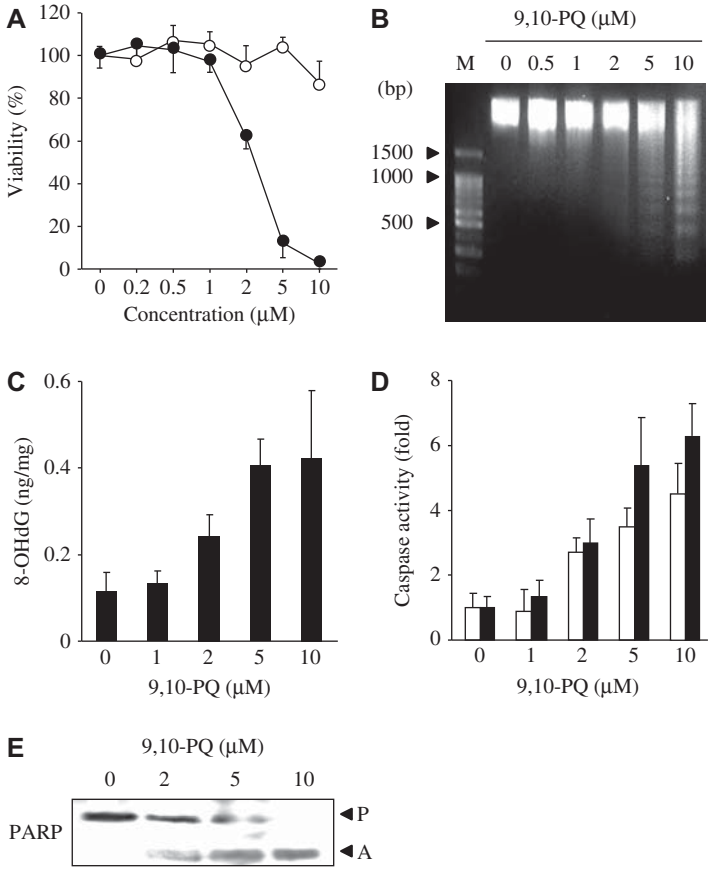

Figure 1. Treatment with 9,10-PQ induces YPEN1 cell apoptosis through a mechanism dependent on enhanced ROS production and caspase activation. (A) Cytotoxicity of 9,10-PQ. The cells were treated for 24 h with the indicated concentrations of phenanthrene (○) or 9,10-PQ (●). Data are expressed as percentages of the viability value in the control cells treated with the vehicle DMSO alone. (B) DNA fragmentation in the cells treated for 24 h with the 9,10-PQ concentrations. DNA was visualized under UV light after staining with ethidium bromide. M: DNA size markers. (C) 8-OHdG formation in the cells treated for 8 h with 0, 1, 2, 5 or 10 μM 9,10-PQ. (D) Activation of caspase-9 (open bar) and caspase-3 (closed bar) in the cells treated for 16 h with 1, 2, 5 or 10 μM 9,10-PQ. The enzyme activities are expressed as the fold increases in the ratio of the activity in the treated cells to that in the control cells (0 μM). (D) PARP cleavage. The cells were treated for 24 h with 0, 2, 5 or 10 μM 9,10-PQ and PARP precursor (P) and its active form (A) in the cell extracts (100 μg) were detected by Western blot analysis using the anti-PARP antibodies.

Measurement of superoxide anion

The level of superoxide anion generated in the reduction of 9,10-PQ by AKR1C15 was determined by the method of McCord and Fridovich [28]. The assay mixture consisted of 0.1 M potassium phosphate buffer, pH 7.4, 0.5 mM NADPH, 0.1 mM EDTA, 50 μM ferricytochrome *c*, 10 μM 9,10-PQ and the enzyme or the cell extract, in a total volume of 2.0 ml. The formation rate of ferrocytochrome *c* at 37°C was spectrophotometrically monitored at 550 nm.

Statistical analysis

Data are expressed as means ± SD of at least three independent experiments, unless otherwise noted. Statistical evaluation of the data was performed by using the unpaired Student's *t*-test and ANOVA followed by Fisher's test. A p-value < 0.05 was considered statistically significant.

Results

9,10-PQ-induced YPEN1 apoptosis through ROS-dependent ER stress

The treatment with 9,10-PQ for 24 h resulted in a dose-dependent decrease in the viability of rat endothelial YPEN1 cells, while the treatment by phenanthrene without the quinone structure had no effect on the viability (Figure 1A). The cytotoxicity was remarkably high at the 9,10-PQ concentration of more than 5 μM, in which the clear fragmentation of DNA, indicative of apoptotic cell death, was observed (Figure 1B). In addition, the treatment with the 9,10-PQ concentration of more than 2 μM facilitated the formation of 8-OHdG, a marker of DNA damage caused by oxidative stress (Figure 1C), and activated caspases (caspase-3 and caspase-9) (Figure 1D) and PARP (Figure 1E). These results suggest that ROS and its downstream effectors (caspases and PARP) are critical to the apoptotic mechanism of the 9,10-PQ-induced damage in

the rat endothelial cells, as well as human-derived cells [17,18].

Since accumulation of ROS is assumed to induce ER stress, we examined whether ER stress is involved in the mechanism of the 9,10-PQ-induced apoptosis of YPEN1 cells. When the amount of CHOP, a pro-apoptotic protein that is induced by ER stress-dependent signalling [29], was monitored upon exposure of YPEN1 cells to 10 μM 9,10-PQ, its pronounced induction was observed at 4 h after the treatment and reached a maximal level (~ 4-fold increase over the basal level) at 24 h (Figure 2A). In addition, the 24 h-treatment with 9,10-PQ concentration > 5 μM resulted in a decrease in the proteolytic (chymotrypsin-like) activity of *26S* proteasome (Figure 2B), which plays a central role in the ER-associated degradation of unfolded proteins [30]. The pre-treatment with MG132, a potent inhibitor of the proteasomal function, also induced CHOP in the cells and synergistically potentiated the 9,10-PQ-induced CHOP expression (Figure 2C). In addition, the pre-treatment with MG132 enhanced the cytotoxicity of 2 μM 9,10-PQ (Figure 2D). Considering that proteasomal function is down-regulated by ROS such as H_2O_2 [31], the above results raise the possibility that 9,10-PQ induces ER stress through the ROS-mediated proteasomal dysfunction. To test this, we examined the effect of the pre-treatment with MG132 on cytotoxicity induced by other ROS-producing compounds (1,2-naphthoquinone [32], 1,4-naphthoquinone [32] and 4HNE [21]) and H_2O_2. The susceptibility of YPEN1 cells to the toxicity of these compounds and H_2O_2 was greatly increased by the MG132 pre-treatment, similar to the case of the 9,10-PQ-induced toxicity. The involvement of ROS in the apoptotic signalling initiated by 9,10-PQ was also validated in almost complete prevention of the MG132-enhanced cytotoxicity by PEG-cat (Figure 2D).

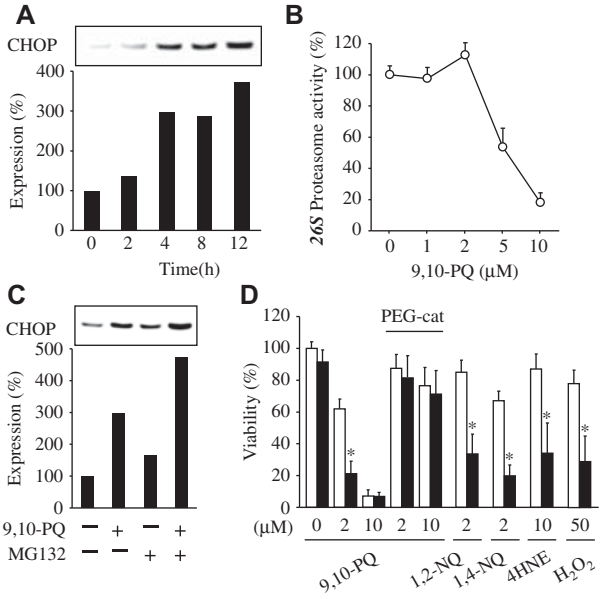

Figure 2. 9,10-PQ treatment causes CHOP induction and proteasomal dysfunction in YPEN1 cells. (A) Time course of CHOP induction. The cells were treated with 10 μM 9,10-PQ for the indicated time and CHOP was detected by Western blotting (upper panel). Lower panel shows the CHOP levels that are expressed as percentages of the band density relative to that in the control cells before the treatment. The values represent the means from two independent experiments. (B) Inactivation of proteasome. The cells were treated for 24 h with 0, 1, 2, 5 or 10 μM 9,10-PQ and the chymotrypsin-like activity of *26S* proteasome in the cell extracts was measured. Data are expressed as percentages relative to the activity in the cells treated with 0 μM 9,10-PQ. (C) Effect of proteasome inhibitor MG132 on CHOP induction by 9,10-PQ. The cells were treated for 24 h with 10 μM 9,10-PQ 12 h after pre-treatment with 50 nM MG132. CHOP levels were determined by Western blotting (upper panel) and are expressed as relative percentages (lower panel). (D) Effect of MG132 on the 9,10-PQ-induced viability loss. The cells were pre-treated for 12 h without (open bar) or with 50 nM MG132 (closed bar) prior to treating for 24 h with the indicated concentrations of 9,10-PQ, 1,2-naphthoquinone (*1,2-NQ*), 1,4-naphthoquinone (*1,4-NQ*), 4HNE or H_2O_2. In the PEG-cat groups, 200 U/ml PEG-cat was added into the culture medium 2 h before the initiation of 9,10-PQ treatment. * Significant difference from the group treated without MG132, $p < 0.05$.

AKR1C15 induces ROS formation via a redox cycling of 9,10-PQ

To assess the involvement of AKR1C15 in the 9,10-PQ-redox cycling, we analysed the products from the *in vitro* NADPH-linked reduction of 9,10-PQ by this enzyme on HPLC (Figure 3A). As shown in the HPLC chromatograms, no peak corresponding to the acetyl derivative (9,10-DAP) of the expected reduced product 9,10-PQH_2 (*peak* 2) was detected in the reaction mixture (Figure 3Ab). Since superoxide anion is generated and involved in the 9,10-PQ-redox cycling [17,18], CuZnSOD was added into the reaction mixture. The reaction in the presence of CuZnSOD formed a new product (Figure 3Ac), which was entirely overlaid with authentic 9,10-DAP (Figure 3Ad). The amount of the resulting 9,10-PQH_2 was increased in a concentration-dependent manner of AKR1C15 added into the reaction mixture containing CuZnSOD (Figure 3B). The production of superoxide anion in the 9,10-PQ-redox cycling mediated by AKR1C15 was also evidenced by the significant decrease in reduction of ferricytochrome *c* by addition of CuZnSOD (Figure 3C).

Involvement of AKR1C15 in 9,10-PQ-induced endothelial cell damage

We investigated the role of AKR1C15 in the endothelial cell damage by 9,10-PQ using the enzyme-over-expressing BAE cells previously established [21]. The AKR1C15-over-expressing cells were apparently susceptible to cytotoxicity of 9,10-PQ (Figure 4A) exhibiting the half-maximal lethal dose (LD_{50}) of 1.1 μM, compared with the control cells (LD_{50} = 1.7 μM). Similarly, the ectopic expression of AKR1C15 in human embryo kidney

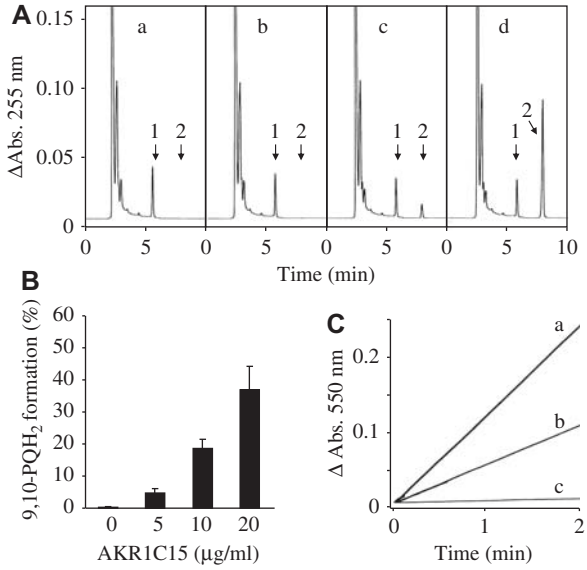

Figure 3. ROS generation in 9,10-PQ reduction by purified AKR1C15. (A) HPLC chromatograms of the products of 9,10-PQ reduction by AKR1C15 (20 μg). The products formed by the incubation for 15 min were acetylated and then followed by detection at 255 nm in the HPLC analysis. Besides some unknown peaks at retention times ~ 2.5 min, only the peak corresponding to 9,10-PQ (retention time; 6.1 min, peak 1) was detected in the complete reaction mixture without (a) or with the enzyme (b). The incubation in the presence of 200 U CuZnSOD (c) yielded an additional product (peak 2), which was identical to the authentic 9,10-DAP as evident by the chromatogram of the mixture of the products of (c) and 200 pmol 9,10-DAP (d). (B) 9,10-PQH_2 formation during 9,10-PQ reduction by AKR1C15. The indicated concentrations of AKR1C15 were incubated for 15 min with the complete reaction mixture in the presence of 200 U CuZnSOD and 9,10-PQH_2 was determined as described in (A). Data are expressed as percentages of 9,10-DAP formed in the reaction mixture to 9,10-PQ before incubation. (C) Cytochrome *c* reduction coupled with 9,10-PQ reduction. AKR1C15 (20 μg) was incubated with ferricytochrome *c* and 10 μM 9,10-PQ in the absence (a) or presence of 200 U CuZnSOD (b). The reduction rate of ferricytochrome *c* was spectrophotometrically monitored at 550 nm. No significant reduction of ferricytochrome *c* was observed without 9,10-PQ (c).

HEK293 cells increased the susceptibility to the quinone cytotoxicity (data not shown). We also examined the effect of the under-expression of AKR1C15 on the quinone cytotoxicity using the AKR1C15-under-expressing phenotype of YPEN1 cells that were prepared by introducing the specific antibodies against the enzyme. Western blot analysis revealed that AKR1C15 non-reacted with the antibodies in the phenotype was ~ 26% of its basal level (data not shown). The AKR1C15-under-expressing cells showed significantly low susceptibility to the 9,10-PQ-induced damage compared with the control cells (Figure 4B).

9,10-PQ increases AKR1C15 expression via Nrf2-dependent signalling

When the expression level of AKR1C15 in YPEN1 cells treated with 9,10-PQ was examined by Western

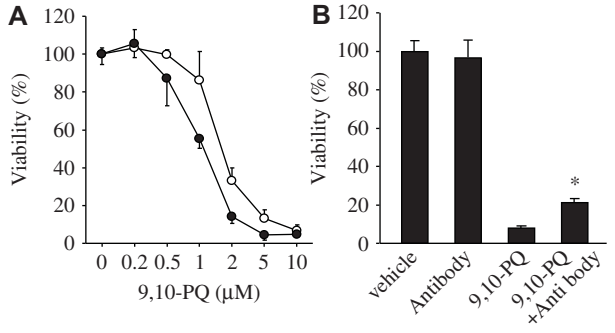

Figure 4. Exacerbation of 9,10-PQ-induced damage by AKR1C15. The damage is expressed as the viability relative to that of the control cells treated with the vehicle DMSO. (A) Effect of over-expression of AKR1C15. BAE cells were transfected for 48 h with the expression vector alone (open circle) or the vector carrying AKR1C15 cDNA (closed circle) and then treated for 24 h with the indicated concentrations of 9,10-PQ. (B) Effect of introduction of anti-AKR1C15 antibody. The control YPEN1 cells (*vehicle*) and antibody-introduced cells (*antibody*) were treated for 24 h without or with 10 μM 9,10-PQ. *Significant difference from the group treated with 9,10-PQ alone, $p < 0.05$.

blotting, we found a marked elevation of the enzyme expression in the cells which were treated with a sub-lethal concentration (0.5 μM) of 9,10-PQ (Figure 5A). The induction of AKR1C15 by 9,10-PQ treatment was also observed in the tissue cultures of rat aorta and heart, in which the enzyme levels were increased ~ 3-fold by 20 μM 9,10-PQ treatment (Figure 5B). As shown in the preceding experiments, the 9,10-PQ treatment enhanced cellular ROS production. The induction of AKR1C15 by 9,10-PQ in YPEN1 cells was depressed by the pre-treatment of PEG-cat (Figure 5A), being indicative of participation of ROS generation in the enzyme induction. ROS generated during exposure to DEP induces phase II xenobiotic metabolizing enzymes including NADPH quinone oxidoreductase-1 through activation of the stress-sensitive Nrf2 transcription factor [33]. To investigate an involvement of the Nrf2-dependent pathway in the induction of AKR1C15 by 9,10-PQ, YPEN1 cells were treated with the potent Nrf2 activators, ethacrynic acid [34] and sulphoraphane [35]. The activators enhanced the expression of AKR1C15, although their concentrations were higher than that of 9,10-PQ (Figure 5C). In addition, the amount of Nrf2 translocated to the nuclei increased ~ 8-fold by the treatment of YPEN1 cells with 0.5 μM 9,10-PQ. These results clearly indicate the involvement of Nrf2 activation in transcriptional regulation of AKR1C15 gene. Furthermore, the pre-treatment of YPEN1 cells with ethacrynic acid potentiated the cytotoxity of 9,10-PQ, supporting the participation of the Nrf2-linked AKR1C15 induction in this toxicity (Figure 5D).

Discussion

In this study, we have demonstrated that treatment of rat endothelial cells with 9,10-PQ elicits apoptosis, in

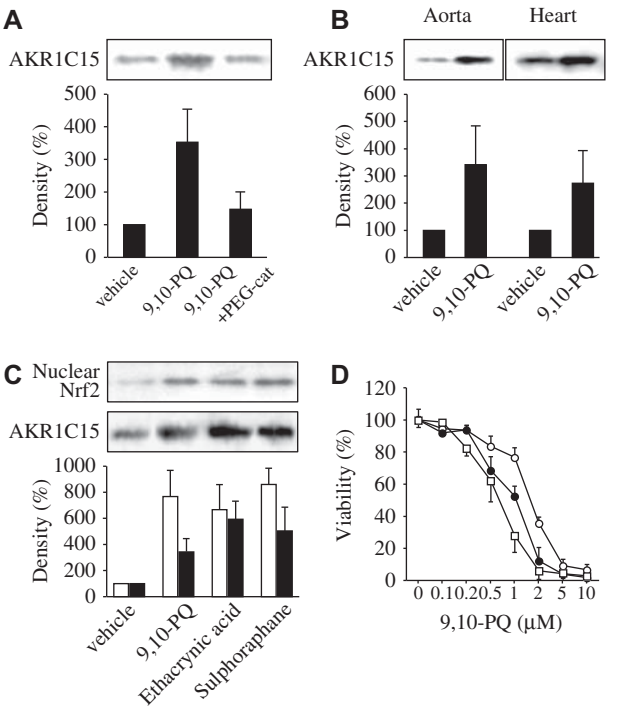

Figure 5. Induction of AKR1C15 by treatment with 9,10-PQ. (A) Effect of 9,10-PQ on AKR1C15 levels. YPEN1 cells and the PEG-cat-pre-treated cells (+ *PEG-cat*) were treated without (*vehicle*) and with 0.5 μM 9,10-PQ (*9,10-PQ*) for 24 h. (B) Change in AKR1C15 level in rat aorta and heart by 9,10-PQ treatment. The cultured cells of rat aortic ring and heart were treated for 24 h with 20 μM 9,10-PQ. (C) Effects of 9,10-PQ and Nrf2 activators on Nrf2 translocation into nucleus and AKR1C15 induction. YPEN1 cells were treated for 24 h with 0.5 μM 9,10-PQ, 10 μM ethacrynic acid or 5 μM sulphoraphane. Protein levels of Nrf2 (□) and AKR1C15 (■) in (A) to (C) were determined by Western blotting as described in the Methods section and are expressed as the expression percentages relative to that in the control group treated with DMSO (*vehicle*). (D) Effect of ethacrynic acid on 9,10-PQ-induced cytotoxicity. YPEN1 cells were pre-treated for 24 h with 0 (○), 2 (●) and 10 μM (□) ethacrynic acid and then treated for 24 h with the indicated concentrations of 9,10-PQ. Data are expressed as percentages of the viability value in the control cells treated with DMSO.

which enhanced ROS generation triggers the mitochondrial dysfunction and activation of caspases and PARP. These 9,10-PQ-induced apoptotic alterations are almost consistent with the results obtained in experiments using human T-lymphocytes and endothelial cells [17,18]. In addition, this study shows, for the first time, the involvement of ER stress in the apoptotic signalling initiated by 9,10-PQ. Considering that incubation with organic extracts from DEP promotes an unfolding protein response in bronchial endothelial cells [36], it is feasible that 9,10-PQ is a predominant component eliciting the ER stress induced by DEP. ER stress is induced by accumulation of unfolded and misfolded proteins and/or dysfunction of proteasome [30,37]. It also activates three distinct sensor proteins, double stranded RNA-activated protein kinase-like ER kinase (PERK), activating transcription factor 6 and inositol-requiring enzyme-1α and 1β. Potent stimulation over capacity to recover from the ER stress induces expression of CHOP, a downstream target of pro-apoptotic signallings dependent on PERK and presumably the other two sensor proteins [38–40]. Our current results have shown that in YPEN1 cells CHOP is markedly elevated at 4 h after initiation of the 9,10-PQ treatment (Figure 2A). Since ROS generation by 9,10-PQ was observed within 3 h in human endothelial cells (unpublished data), the excess ROS by 9,10-PQ may provoke ER stress including the CHOP induction. Consistent with our suggestion, several reports also indicated that ROS disrupts ER homeostasis resulting in up-regulation of CHOP [37,40–44]. Here we have indicated that 9,10-PQ treatment causes proteasome dysfunction in rat endothelial cells (Figure 2B). The proteasomal inactivation is most likely due to accumulation of ROS according to our previous report [31]. Because inhibition of proteasome elevates intracellular ROS level [45], ROS may serve as a negative feedback inhibition of proteasome function, resulting in exacerbation of ER stress and the following apoptotic initiation. The ROS-dependent increase in CHOP level is reported to be mediated by activations of p38 MAPK [46] and c-Jun N-terminal kinase [47]. In addition, we propose that the proteasomal inactivation caused by ROS is a major mechanism of the enhanced CHOP expression caused by incubation with 9,10-PQ. The proposal is obvious from the results that the CHOP induction by 9,10-PQ is augmented by proteasomal inactivation (Figure 2C) and that the removal of intracellular ROS by PEG-cat resulted in an almost complete restoration of the MG132-induced sensitization to the quinone (Figure 2D). CHOP is known to down-regulate an anti-apoptotic mitochondrial protein bcl-2 [48] and to translocate a pro-apoptotic protein bax into mitochondria [49], leading to reduction of mitochondrial membrane potential. CHOP may, therefore, be a pivotal signalling molecule that causes the above-mentioned ROS-dependent apoptotic alterations (mitochondrial dysfunction and caspase activation) in response to 9,10-PQ.

We have provided direct evidence that in rat endothelial cells AKR1C15 is a key reductase that enhances the redox cycling of 9,10-PQ, resulting in ROS production (Figure 3). The above suggests that AKR1C15 may play a central role in the early stage of mechanism(s) underlying the 9,10-PQ-induced apoptosis of various rat cells expressing the enzyme. Because AKR1C15 is highly expressed in rat lung cells such as pulmonary alveolar type II and bronchiolar (Clara) epithelial cells as well as the vascular endothelial cells [20], the enzyme is probably involved in pulmonary abnormalities observed in DEP-challenged rats [50,51]. Among the rat AKR1C subfamily members other than AKR1C15, AKR1C9 is known to effectively catalyse the NADPH-dependent reduction of 9,10-PQ. Based on the results by Schlegel et al. [52], the catalytic

efficiency of AKR1C9 towards the toxic quinone is equal to or higher than that of AKR1C15. Additionally, analyses of *in vitro* enzymatic reaction and RT-PCR showed that a rat aldose reductase-like protein, AKR1B13, acts as a quinone reductase in vascular cells including endothelial cells (data not shown). It would be interesting to elucidate the involvement of the two candidate enzymes in the 9,10-PQ damage and to compare with that of AKR1C15. In experiments using AKR1C15-over-expressing cells, the enzyme augmented the 9,10-PQ-induced cell damage (Figure 4A), despite having a capacity to detoxify some lipid peroxides, particularly 4HNE, formed by oxidative stress [21]. The augmentation may be due to high catalytic efficiency of AKR1C15 for 9,10-PQ, leading to high production of ROS beyond its cytoprotective capacity. The abundant production of ROS during exposure to 9,10-PQ then elicits decreases in levels of antioxidant-related enzymes (CuZnSOD and hemeoxygenase-1) and intracellular reduced glutathione [11 and unpublished data]. Thus, AKR1C15 functions as a key regulator for mediating cellular effects of the preferred substrates, 9,10-PQ and 4HNE.

Accumulation of ROS is thought to modulate expression of phase II metabolic enzymes *via* an Nrf2-dependent signalling [53,54]. Under basal conditions, Nrf2 exists in the cell cytosol complexed with an Nrf2 inhibitor, Kelch-like ECH-associated protein 1 (Keap1) and undergoes degradation by ubiquitin/proteasome system. Upon stimulation by ROS and electrophiles, Nrf2 is dissociated from Keap1 by the modification of thiol groups in cysteine residues [55]. Nrf2 then translocates into the nucleus, where it accelerates transcription of antioxidant response element-responsive genes, such as NADPH:quinone oxidereductase, hemeoxygenase-1 and γ-glutamylcysteine ligase. In addition to the cytoprotective enzymes, some human AKR members (AKR1B10, AKR1C1, AKR1C2 and AKR1C3) have been reported to be transcriptionally activated in the Nrf2-mediated pathway [56]. In our current study, low concentration of 9,10-PQ elevated expression of AKR1C15 through the enhanced ROS production, as evident from the results on Western blotting of AKR1C15 (Figure 5A). To our knowledge, this is the first report demonstrating that treatment with 9,10-PQ activates the Nrf2 pathway in endothelial cells. The AKR1C15 induction by ROS is in agreement with our previous reports [21,57]. Assuming that, like the genes for the human members of the AKR superfamily, the AKR1C15 gene is regulated by the Nrf2-dependent signalling, it is reasonable to enhance the enzyme level by treatment with ethacrynic acid or sulphoraphane alone. The assumption is also supported by our preliminary data showing that the 9,10-PQ treatment (0.5 μM) increased message of an Nrf2-related protein hemeoxygenase-1 in YPEN1 cells. Inhibition of proteasome function is thought to cause accumulation of undegraded Nrf2 in cells. Therefore, the MG132-mediated cell sensitization against the 9,10-PQ toxicity (Figure 2C) may be in part due to induction of AKR1C15 by the accumulated Nrf2. Previous investigation using human lung cancer A549 cells and primary hepatocyte from Nrf2-knockout mouse found that some Nrf2-derived enzymes such as UDP-glucuronosyltransferases and multidrug resistance proteins promote glucuronidation of 9,10-PQH_2 and the excretion into extracellular space [58]. In contrast, our cytotoxicity assay revealed that AKR1C15 newly induced by 9,10-PQ also participated in the quinone toxicity in rat endothelial cells (Figure 5D). This apparent contradiction might be explained by difference in expression levels of the metabolizing enzymes among the cells used in the experiments. Thus, 9,10-PQ induces AKR1C15 expression presumably via an Nrf2-dependent pathway and ROS production in the metabolic cycle undergone by the induced enzyme, both of which are closely associated with the formation of a negative feedback loop exacerbating a cytotoxic effect of the quinone on rat endothelial cells.

Acknowledgements

This work was supported in part by a grant for encouragement of young scientists from Gifu Pharmaceutical University.

Declaration of interest

The authors report no conflicts of interest. The authors alone are responsible for the content and writing of the paper.

References

[1] Schwela D. Air pollution and health in urban areas. Rev Environ Health 2000;15:13–42.
[2] Delfino RJ. Epidemiologic evidence for asthma and exposure to air toxics: linkages between occupational, indoor, and community air pollution research. Environ Health Perspect 2002;110:573–589.
[3] Polosa R, Salvi S, Di Maria GU. Allergic susceptibility associated with diesel exhaust particle exposure: clear as mud. Arch Environ Health 2002;57:188–193.
[4] Nemmar A, Hoylaerts MF, Hoet PH, Nemery B. Possible mechanisms of the cardiovascular effects of inhaled particles: systemic translocation and prothrombotic effects. Toxicol Lett 2004;149:243–253.
[5] Yu CP, Xu GB. Predictive models for deposition of inhaled diesel exhaust particles in humans and laboratory species. Res Rep Health Eff Inst 1987;10:3–22.
[6] Sagai M, Furuyama A, Ichinose T. Biological effects of diesel exhaust particles (DEP). III. Pathogenesis of asthma like symptoms in mice. Free Radic Biol Med 1996;21:199–209.
[7] Bai Y, Suzuki AK, Sagai M. The cytotoxic effects of diesel exhaust particles on human pulmonary artery endothelial cells *in vitro*: role of active oxygen species. Free Radic Biol Med 2001;30:555–562.

[8] Nemmar A, Hoet PH, Vanquickenborne B, Dinsdale D, Thomeer M, Hoylaerts MF, et al. Passage of inhaled particles into the blood circulation in humans. Circulation 2002;105: 411–414.
[9] Cassee FR, Boere AJ, Bos J, Fokkens PH, Dormans JA, van Loveren H. Effects of diesel exhaust enriched concentrated PM2.5 in ozone preexposed or monocrotaline-treated rats. Inhal Toxicol 2002;14:721–743.
[10] Bérubé KA, Jones TP, Williamson BJ. Electron microscopy of urban airborn particulate matter. Microsc Anal 1997;49:9–11.
[11] Sugimoto R, Kumagai Y, Nakai Y, Ishii T. 9,10-Phenanthraquinone in diesel exhaust particles downregulates Cu,Zn-SOD and HO-1 in human pulmonary epithelial cells: intracellular iron scavenger 1,10-phenanthroline affords protection against apoptosis. Free Radic Biol Med 2005;38:388–395.
[12] Jarabak J. Polycyclic aromatic hydrocarbon quinone-mediated oxidation reduction cycling catalyzed by a human placental NADPH-linked carbonyl reductase. Arch Biochem Biophys 1991;291:334–338.
[13] Oginuma M, Shimada H, Imamura Y. Involvement of carbonyl reductase in superoxide formation through redox cycling of adrenochrome and 9,10-phenanthrenequinone in pig heart. Chem Biol Interact 2005;155:148–154.
[14] Taguchi K, Fujii S, Yamano S, Cho AK, Kamisuki S, Nakai Y, et al. An approach to evaluate two-electron reduction of 9,10-phenanthraquinone and redox activity of the hydroquinone associated with oxidative stress. Free Radic Biol Med 2007;43:789–799.
[15] Chesis PL, Levin DE, Smith MT, Ernster L, Ames BN. Mutagenicity of quinones: pathways of metabolic activation and detoxification. Proc Natl Acad Sci USA 1984;81:1696–1700.
[16] Kumagai Y, Arimoto T, Shinyashiki M, Shimojo N, Nakai Y, Yoshikawa T, Sagai M. Generation of reactive oxygen species during interaction of diesel exhaust particle components with NADPH-cytochrome P450 reductase and involvement of the bioactivation in the DNA damage. Free Radic Biol Med 1997; 22:479–487.
[17] Matsunaga T, Kamiya T, Sumi D, Kumagai Y, Kalyanaraman B, Hara A. L-Xylulose reductase is involved in 9,10-phenanthrenequinone-induced apoptosis in human T lymphoma cells. Free Radic Biol Med 2008;44:1191–1202.
[18] Matsunaga T, Arakaki M, Kamiya T, Endo S, El-Kabbani O, Hara A. Involvement of an aldo-keto reductase (AKR1C3) in redox cycling of 9,10-phenanthrenequinone leading to apoptosis in human endothelial cells. Chem Biol Interact 2009;181:52–60.
[19] Matsunaga T, Shintani S, Hara A. Multiplicity of mammalian reductases for xenobiotic carbonyl compounds. Drug Metab Pharmacokinet 2006;21:1–18.
[20] Endo S, Matsunaga T, Horie K, Tajima K, Bunai Y, Carbone V, et al. Enzymatic characteristics of an aldo-keto reductase family protein (AKR1C15) and its localization in rat tissues. Arch Biochem Biophys 2007;465:136–147.
[21] Matsunaga T, Shinoda Y, Inoue Y, Endo S, El-Kabbani O, Hara A. Protective effect of rat aldo-keto reductase (AKR1C15) on endothelial cell damage elicited by 4-hydroxy-2-nonenal. Chem Biol Interact 2011; in press.
[22] Domenighetti AA, Bény JL, Chabaud F, Frieden M. An intercellular regenerative calcium wave in porcine coronary artery endothelial cells in primary culture. J Physiol 1998;513: 103–116.
[23] Usui S, Matsunaga T, Ukai S, Kiho T. Growth suppressing activity for endothelial cells induced from macrophages by carboxymethylated curdlan. Biosci Biotechnol Biochem 1997;61:1924–1925.
[24] Kotamraju S, Konorev EA, Joseph J, Kalyanaraman B. Doxorubicin-induced apoptosis in endothelial cells and cardiomyocytes is ameliorated by nitrone spin traps and ebselen. Role of reactive oxygen and nitrogen species. J Biol Chem 2000;275:33585–33592.
[25] Matsunaga T, Kotamraju S, Kalivendi SV, Dhanasekaran A, Joseph J, Kalyanaraman B. Ceramide-induced intracellular oxidant formation, iron signaling, and apoptosis in endothelial cells: protective role of endogenous nitric oxide. J Biol Chem 2004;279:28614–28624.
[26] Thomas S, Kotamraju S, Zielonka J, Harder DR, Kalyanaraman B. Hydrogen peroxide induces nitric oxide and proteosome activity in endothelial cells: a bell-shaped signaling response. Free Radic Biol Med 2007;42:1049–1061.
[27] Mohan S, Mohan N, Sprague EA. Differential activation of NF-kappa B in human aortic endothelial cells conditioned to specific flow environments. Am J Physiol 1997;273:C572–C578.
[28] McCord JM, Fridovich I. Superoxide dismutase. An enzymic function for erythrocuprein (hemocuprein). J Biol Chem 1969;244:6049–6055.
[29] Wang XZ, Lawson B, Brewer JW, Zinszner H, Sanjay A, Mi LJ, et al. Signals from the stressed endoplasmic reticulum induce C/EBP-homologous protein (CHOP/GADD153). Mol Cell Biol 1996;16:4273–4280.
[30] Schröder M, Kaufman RJ. The mammalian unfolded protein response. Annu Rev Biochem 2005;74:739–789.
[31] Matsunaga T, Arakaki M, Kamiya T, Haga M, Endo S, El-Kabbani O, Hara A. Nitric oxide mitigates apoptosis in human endothelial cells induced by 9,10-phenanthrenequinone: role of proteasomal function. Toxicology 2010;268:191–197.
[32] Lin PH, Pan WC, Kang YW, Chen YL, Lin CH, Lee MC, et al. Effects of naphthalene quinonoids on the induction of oxidative DNA damage and cytotoxicity in calf thymus DNA and in human cultured cells. Chem Res Toxicol 2005;18:1262–1270.
[33] Baulig A, Garlatti M, Bonvallot V, Marchand A, Barouki R, Marano F, Baeza-Squiban A. Involvement of reactive oxygen species in the metabolic pathways triggered by diesel exhaust particles in human airway epithelial cells. Am J Physiol Lung Cell Mol Physiol 2003;285:L671–L679.
[34] Wu RP, Hayashi T, Cottam HB, Jin G, Yao S, Wu CC, et al. Nrf2 responses and the therapeutic selectivity of electrophilic compounds in chronic lymphocytic leukemia. Proc Natl Acad Sci USA 2010;107:7479–7484.
[35] Morimitsu Y, Nakagawa Y, Hayashi K, Fujii H, Kumagai T, Nakamura Y, et al. A sulforaphane analogue that potently activates the Nrf2-dependent detoxification pathway. J Biol Chem 2002;277:3456–3463.
[36] Jung EJ, Avliyakulov NK, Boontheung P, Loo JA, Nel AE. Pro-oxidative DEP chemicals induce heat shock proteins and an unfolding protein response in a bronchial epithelial cell line as determined by DIGE analysis. Proteomics 2007;7:3906–3918.
[37] Wu J, Kaufman RJ. From acute ER stress to physiological roles of the Unfolded Protein Response. Cell Death Differ 2006;13:374–384.
[38] Ma Y, Brewer JW, Diehl JA, Hendershot LM. Two distinct stress signaling pathways converge upon the CHOP promoter during the mammalian unfolded protein response. J Mol Biol 2002;318:1351–1365.
[39] Gotoh T, Oyadomari S, Mori K, Mori M. Nitric oxide-induced apoptosis in RAW 264.7 macrophages is mediated by endoplasmic reticulum stress pathway involving ATF6 and CHOP. J Biol Chem 2002;277:12343–12350.
[40] Xu C, Bailly-Maitre B, Reed JC. Endoplasmic reticulum stress: cell life and death decisions. J Clin Invest 2005;115: 2656–2664.
[41] Tagawa Y, Hiramatsu N, Kasai A, Hayakawa K, Okamura M, Yao J, Kitamura M. Induction of apoptosis by cigarette smoke via ROS-dependent endoplasmic reticulum stress and CCAAT/enhancer-binding protein-homologous protein (CHOP). Free Radic Biol Med 2008;45:50–59.
[42] Sekine Y, Takeda K, Ichijo H. The ASK1-MAP kinase signaling in ER stress and neurodegenerative diseases. Curr Mol Med 2006;6:87–97.
[43] Yokouchi M, Hiramatsu N, Hayakawa K, Okamura M, Du S, Kasai A, et al. Involvement of selective reactive oxygen species

upstream of proapoptotic branches of unfolded protein response. J Biol Chem 2008;283:4252–4260.
[44] Adachi M, Liu Y, Fujii K, Calderwood SK, Nakai A, Imai K, Shinomura Y. Oxidative stress impairs the heat stress response and delays unfolded protein recovery. PLoS One 2009; 4:e7719.
[45] Fribley A, Zeng Q, Wang CY. Proteasome inhibitor PS-341 induces apoptosis through induction of endoplasmic reticulum stress-reactive oxygen species in head and neck squamous cell carcinoma cells. Mol Cell Biol 2004;24: 9695–9704.
[46] Wang XZ, Ron D. Stress-induced phosphorylation and activation of the transcription factor CHOP (GADD153) by p38 MAP Kinase. Science 1996;272:1347–1349.
[47] Kültz D, Madhany S, Burg MB. Hyperosmolality causes growth arrest of murine kidney cells. Induction of GADD45 and GADD153 by osmosensing via stress-activated protein kinase 2. J Biol Chem 1998;273:13645–13651.
[48] Matsumoto M, Minami M, Takeda K, Sakao Y, Akira S. Ectopic expression of CHOP (GADD153) induces apoptosis in M1 myeloblastic leukemia cells. FEBS Lett 1996;395: 143–147.
[49] Gotoh T, Terada K, Oyadomari S, Mori M. hsp70-DnaJ chaperone pair prevents nitric oxide- and CHOP-induced apoptosis by inhibiting translocation of Bax to mitochondria. Cell Death Differ 2004;11:390–402.
[50] Mauderly JL, Jones RK, Griffith WC, Henderson RF, McClellan RO. Diesel exhaust is a pulmonary carcinogen in rats exposed chronically by inhalation. Fundam Appl Toxicol 1987;9:208–221.
[51] Arimoto T, Kadiiska MB, Sato K, Corbett J, Mason RP. Synergistic production of lung free radicals by diesel exhaust particles and endotoxin. Am J Respir Crit Care Med 2005; 171:379–387.
[52] Schlegel BP, Ratnam K, Penning TM. Retention of NADPH-linked quinone reductase activity in an aldo-keto reductase following mutation of the catalytic tyrosine. Biochemistry 1998;37:11003–11011.
[53] Zhang DD. Mechanistic studies of the Nrf2-Keap1 signaling pathway. Drug Metab Rev 2006;38:769–789.
[54] Kaspar JW, Niture SK, Jaiswal AK. Nrf2: INrf2 (Keap1) signaling in oxidative stress. Free Radic Biol Med 2009; 47:1304–1309.
[55] Dinkova-Kostova AT, Holtzclaw WD, Cole RN, Itoh K, Wakabayashi N, Katoh Y, et al. Direct evidence that sulfhydryl groups of Keap1 are the sensors regulating induction of phase 2 enzymes that protect against carcinogens and oxidants. Proc Natl Acad Sci USA 2002;99:11908–11913.
[56] MacLeod AK, McMahon M, Plummer SM, Higgins LG, Penning TM, Igarashi K, Hayes JD. Characterization of the cancer chemopreventive NRF2-dependent gene battery in human keratinocytes: demonstration that the KEAP1-NRF2 pathway, and not the BACH1-NRF2 pathway, controls cytoprotection against electrophiles as well as redox-cycling compounds. Carcinogenesis 2009;30:1571–1580.
[57] Endo S, Matsunaga T, Mamiya H, Hara A, Kitade Y, Tajima K, El-Kabbani O. Characterization of a rat NADPH-dependent aldo-keto reductase (AKR1B13) induced by oxidative stress. Chem Biol Interact 2009;178:151–157.
[58] Taguchi K, Shimada M, Fujii S, Sumi D, Pan X, Yamano S, et al. Redox cycling of 9,10-phenanthraquinone to cause oxidative stress is terminated through its monoglucuronide conjugation in human pulmonary epithelial A549 cells. Free Radic Biol Med 2008;44:1645–1655.

This paper was first published online on Early Online on 1 June 2011.